great-ring pathway through the pyrrolenine ring. Table IV includes comparison bond orders for a Pariser–Parr–Pople calculation of H_2P.[36] Presumably increased outer-ring current would be manifested by the bond orders $C_1–C_2$ and $C_2–C_3$ coming closer to the average bond order for the 18-membered great ring while the bond order $X–C_3$ (X = S or Se) becomes much smaller. No such clear trends appear in the bond-order data.

The calculations offer another explanation for the observed δ value shifts: i.e., the change in charge of the hydrogen atoms listed in Table V. It can be seen that the H_1 and H_3 atoms are distinctly less positive in S_2TPP than in Se_2TPP, implying greater shielding (i.e., smaller δ value) in S_2TPP.

Summary Discussion

The emission data and theoretical analysis by the IEH model on S_2TPP, $SSeTPP$, and Se_2TPP have led to several conclusions: (1) The Se compounds but not S_2TPP contain an allowed low-energy charge-transfer band $Se(4p_y) \rightarrow b_{2g}$- (π^*). This excited state explains the lack of emission in the Se complexes and is apparent when the first absorption band is curve fit by Gaussians. (2) The calculations suggest the possibility that Se_2TPP^+ may be either a π or a $Se(\sigma^*)$ radical. While Fajer and Richardson[28] believe that their Se_2TPP^+ is a π radical, we believe that their data may also be interpreted as a $Se(\sigma^*)$ radical. In any event, it may be possible to find both types of radical under the proper conditions. (3) The X-ray structures of these species[5] can only be understood if contracted d orbitals are included in the IEH calculations; for only then do the calculations show increased bonding between the group 6 atoms across the core in the order $S_2P < SSeP < Se_2P$. (4) Bond-order analysis of the conjugative pathway does not support the view that the shift to higher δ values of

the thiophene and selenophene exo protons is due to a shift of the ring current from the inner to the outer rings;[1] possibly charge density differences may account for this phenomenon.

The most compelling study that would confirm or refute our view would be a polarized absorption study of the far-red absorption band of these compounds. Such study should show z-polarized absorption in the red tail of $SSeTPP$ and Se_2TPP but not in S_2TPP or the protonated species, where z-polarized absorption may appear further to the blue. Although we found no evidence for phosphorescence, the triplet state should be populated in S_2TPP and its acid dication, both of which show fluorescence. The triplet state may not be populated in $SSeTPP$ and Se_2TPP, where decay to the ground state passes through a charge-transfer state. Transient absorption studies are necessary if a long-lived triplet state is to be found. Finally we note that the study of $^{33}S_2TPP^+$ could provide confirmation of our hypothesis that the unpaired electrons in S_2TPP^+ and in Se_2TPP^+ are in different orbitals.

(36) Weiss, C.; Kobayashi, H.; Gouterman, M. *J. Mol. Spectrosc.* **1965**, *16*, 415.

Contribution from the Department of Chemistry and the Chemical Physics Program, Washington State University, Pullman, Washington 99164

Electronic Spectroscopy of Diphosphine and Diarsine Complexes of Rhodium(I) and Iridium(I)

W. A. FORDYCE and G. A. CROSBY*

The electronic absorption spectra at room temperature, emission and excitation spectra at 77 K, and emission lifetimes at 77 K have been measured for complexes with the general formulas $[M(L–L)_2]^+$ and $[M(L–L)(1,5\text{-cyclooctadiene})]^+$ [M = Rh(I), Ir(I); L–L = diphosphines, diarsine, mixed phosphine–arsine]. For a given metal, the absorption and excitation band energies are relatively insensitive to all the ligands except 1,5-cyclooctadiene. The $\sim 2500\text{-cm}^{-1}$ red shift of the spectral features of the comlexes containing 1,5-cyclooctadiene is attributed to destabilization of all the d orbitals due to closer approach of the diphosphine ligand to the metal center. The low-temperature (1.8–90 K) emission spectral and lifetime data are interpreted in terms of a two-level spin–orbit split triplet manifold. The charge-transfer vs. metal-localized character of the low-energy excited states is discussed.

Introduction

The electronic spectroscopy of Rh(I) and Ir(I) complexes containing ligands such as CO, CN^-, CNR, AsR_3, PR_3, and bidentate diphosphines has been the subject of numerous reports.[1–8] Prototypes for these studies are $[M(L–L)_2]^+$ ions

[M = Rh(I), Ir(I); L–L = diphos or 2≡phos[9]], whose intense photoluminescence and that of complexes containing other

(1) Brady, R.; Miller, M. V.; Vaska, L. *J. Chem. Soc., Chem. Commun.* **1974**, 393.
(2) Geoffroy, G. L.; Wrighton, M. S.; Hammond, G. S.; Gray, H. B. *J. Am. Chem. Soc.* **1974**, *96*, 3105.

(3) Isci, H.; Mason, W. R. *Inorg. Chem.* **1975**, *14*, 913.
(4) Brady, R.; Flynn, B. R.; Geoffroy, G. L.; Gray, H. B.; Peone, J.; Vaska, L. *Inorg. Chem.* **1976**, *15*, 1485.
(5) Geoffroy, G. L.; Isci, H.; Litrenti, J.; Mason, W. R. *Inorg. Chem.* **1977**, *16*, 1950.
(6) Andrews, L. J. *Inorg. Chem.* **1978**, *17*, 3180.
(7) Andrews, L. J. *J. Phys. Chem.* **1979**, *83*, 3203.
(8) Fordyce, W. A.; Rau, H.; Stone, M. L.; Crosby, G. A. *Chem. Phys. Lett.* **1981**, *77*, 405.

Table I. Analyses of Complexes

complex	anal. found (calcd)			
	% C	% H	% P	% As
[Rh(2=phos)$_2$]ClO$_4$	62.66 (62.75)	4.60 (4.47)	12.49 (12.45)	
[Rh(dpbe)$_2$]ClO$_4$	65.50 (65.79)	4.71 (4.43)	10.06 (11.31)	
[Rh(dpp)$_2$]PF$_6$	59.32 (60.45)	5.12 (4.90)	14.61 (14.43)	
[Rh(dcpe)$_2$]PF$_6$	55.98 (57.13)	8.59 (8.87)	13.96 (14.16)	
[Rh(arphos)$_2$]PF$_6$	54.78 (55.14)	4.58 (4.28)	8.98 (8.20)	12.33 (13.23)
[Rh(2=ars)$_2$]PF$_6$	48.95 (51.34)	3.88 (3.65)		22.66 (24.63)
[Rh(2=phos)(cod)]PF$_6$	54.67 (54.27)	4.58 (4.83)	12.43 (12.35)	
[Ir(2=phos)$_2$]ClO$_4$	56.67 (57.59)	4.57 (4.10)	11.29 (11.42)	
[Ir(dpbe)$_2$]ClO$_4$	59.69 (60.83)	4.34 (4.09)	9.24 (10.45)	
[Ir(arphos)$_2$]PF$_6$^{a}	49.39 (51.11)	4.05 (3.96)	7.02 (7.61)	
[Ir(diphos)(cod)]PF$_6$	48.10 (48.39)	4.24 (4.31)	12.93 (11.01)	
[Ir(2=phos)(cod)]PF$_6$	48.28 (48.51)	4.11 (4.08)	9.46 (11.04)	
[Ir(dpbe)(cod)]PF$_6$·CH$_2$Cl$_2$	47.81 (47.95)	3.94 (3.93)	8.94 (9.51)	

^{a} Solid was quite air sensitive; samples stored under argon showed decomposition after 1–2 weeks.

diphosphine and diarsine ligands were first noted by Brady et al.[1] Geoffroy et al. examined their absorption, emission, and emission excitation spectroscopy[2] and magnetic circular dichroism.[5] Subsequently, Andrews measured the excitation polarization[6] and investigated the radiationless decay processes at temperatures above 77 K.[7] Recently we reported the effect of temperature (<77 K) upon their emission band shapes and lifetimes.[8] The principal low-energy bands are generally viewed as metal to ligand charge transfer ($nd_{z^2} \rightarrow \pi_L$) with some admixture of $(n + 1)p_z$ character in the π_L-acceptor molecular orbital. Determination of the extent of this admixture may be important to understand the rich oxidative addition chemistry of these species. Unfortunately, however, investigation of this question is not amenable to spectroscopic techniques that discriminate by symmetry such as magnetic circular dichroism and polarization ratio spectroscopy since the symmetries of both types of orbitals are identical.

We have prepared a series of Rh(I) and Ir(I) complexes containing chelated diphosphine, diarsine, and phosphine-arsine ligands, [M(L–L)$_2$]$^+$ and [M(L–L)(cod)]$^+$ (cod = 1,5-cyclooctadiene), and have attempted to correlate structural changes with spectroscopic trends derived from data on electronic absorption (at room temperature), emission (1.8–77 K), and emission excitation (77 K). The results have been used to quantify the low-energy states and to assess their orbital characteristics.

Experimental Section

Materials. Abbreviations for the complexes and ligands discussed in this paper are given in ref 9. [RhCl(CO)$_2$]$_2$ was obtained from Strem Chemicals, Inc. [RhCl(cod)]$_2$,[10] [IrCl(cod)]$_2$,[11] and [IrCl(cyclooctene)$_2$]$_2$[11] were prepared by published procedures. Phosphine and arsine ligands were obtained from Strem Chemicals, Inc., except *cis*-1,2-bis(diphenylarsino)ethylene, which was prepared by the method of Aguir et al.[12] Microanalyses were performed by Galbraith Laboratories, Inc.

[M(2=phos)$_2$]Cl complexes were prepared by using Vaska and Catone's procedure[13] and then metathesized to the perchlorate salts according to the method of Geoffroy et al.[2] The dpbe analogues were prepared in the same manner and the Ir(I) salt was recrystallized at

room temperature from dichloromethane–diethyl ether. [Rh(2=ars)$_2$]PF$_6$ was prepared from [RhCl(CO)$_2$]$_2$ by the method of Aguir et al.,[12] with the substitution of NH$_4$PF$_6$ for NaBF$_4$. [Rh(arphos)$_2$]PF$_6$, [Rh(dpp)$_2$]PF$_6$ (refluxed in 1-propanol for 30 min), [Rh(dcpe)$_2$]PF$_6$ (no reflux), and [Ir(arphos)$_2$]PF$_6$ (from [IrCl(cyclooctene)$_2$]$_2$ as starting material) were prepared in a similar manner.

The complexes [M(L–L)(cod)]$^+$ (L–L = diphos, 2=phos, dpbe) were prepared by a method described by Schrock and Osborn.[14] In a typical preparation 0.1 g (0.4 mmol) of AgPF$_6$ in 1 mL of ethanol was added to 0.2 mmol of [MCl(cod)]$_2$ in 2 mL of ethanol under argon. AgCl was filtered off, and 0.4 mmol of diphosphine ligand was added to the yellow solution. The mixture was stirred for 10 min, filtered, and washed with benzene and diethyl ether yielding orange [M = Rh(I)] or dark red [M = Ir(I)] products. Typical yields were 0.15 mmol. The Ir(I) salts were subsequently recrystallized at room temperature in dichloromethane–diethyl ether.

Spectroscopy. The solvents used in the spectroscopic studies were spectroscopic grade or distilled before use. The measurements on the [Rh(L–L)$_2$]PF$_6$ (L–L = dpp, arphos, and 2=ars) complexes and all the Ir(I) species were carried out in freeze–pump–thawed solvents. Absorption spectra were taken in dichloromethane solution. Glasses for other spectral measurements were prepared by first dissolving the complex in one part dichloromethane and then adding 20 parts of 4:1 ethanol–methanol. Absorption spectra were measured at room temperature on a Cary 14 spectrophotometer. Emission excitation spectra were obtained with a Hitachi MPF-2A spectrofluorimeter and corrected for monochromator efficiency and lamp intensity variations. Emission spectra were recorded with a red-sensitive spectrophotometer constructed in this laboratory and described earlier[15] except that the lock-in detection system was replaced by dc detection and computer averaging. Sample temperature (other than 77 K) was controlled in an Andonian Model 0-24/7 M-H Dewar described previously.[16] All emission spectra were corrected for monochromator and photomultiplier efficiency.

Decay times were obtained by exciting the sample with a Molectron UV-22 nitrogen laser. The emitted light was filtered through a KNO$_2$ solution, monitored with a RCA photomultiplier wired for fast response,[17] and displayed on a Tektronix 549 oscilloscope. Lifetimes were determined by a linear least-squares fit of ln intensity vs. time. At all temperatures no deviations from exponential behavior were detected over a period of at least 2 lifetimes. Sample temperature was controlled as described above.

Data acquisition and computations were accomplished with a Digital 11/34 system. Spectra were plotted on a Tektronix 4662 digital plotter.

Results

Synthesis. The data in Table I show that the analytical results for a number of compounds exceed generally accepted limits. Multiple analyses on samples from the same preparation often gave values that varied in % C and % P by 1% or 2%. All preparations yielded crystalline products that

(9) M = Rh(I), Ir(I). L–L = Ph$_2$PCH$_2$CH$_2$PPh$_2$, 1,2-bis(diphenylphosphino)ethane (diphos); Ph$_2$PCHCHPPh$_2$, *cis*-1,2-bis(diphenylphosphino)ethylene (2=phos); Ph$_2$PC$_6$H$_4$PPh$_2$, 1,2-bis(diphenylphosphino)benzene (dpbe); Ph$_2$PCH$_2$CH$_2$CH$_2$PPh$_2$, 1,3-bis(diphenylphosphino)propane (dpp); (C$_6$H$_{11}$)$_2$PCH$_2$CH$_2$P(C$_6$H$_{11}$)$_2$, 1,2-bis(dicyclohexylphosphino)ethane (dcpe); Ph$_2$PCH$_2$CH$_2$AsPh$_2$, 1-(diphenylphosphino)-2-(diphenylarsino)ethane (arphos); Ph$_2$AsCHCHAsPh$_2$, 1,2-bis(diphenylarsino)ethylene (2=ars); cod = 1,5-cyclooctadiene.
(10) Chatt, J.; Venanzi, L. M. *J. Chem. Soc.* **1957**, 4735.
(11) Herde, J. L.; Lambert, J. C.; Senoff, C. V. *Inorg. Synth.* **1974**, *15*, 18.
(12) Aguir, A. M.; Mague, J. T.; Aguir, H. J.; Archibald, T. G.; Prejean, G. *J. Org. Chem.* **1968**, *33*, 1681.
(13) Vaska, L.; Catone, D. L. *J. Am. Chem. Soc.* **1966**, *88*, 5324.

(14) Schrock, R. R.; Osborn, J. A. *J. Am. Chem. Soc.* **1971**, *93*, 3089.
(15) Carstens, D. H. W.; Crosby, G. A. *J. Mol. Spectrosc.* **1970**, *34*, 113.
(16) Harrigan, R. W.; Crosby, G. A. *J. Chem. Phys.* **1973**, *59*, 3468.
(17) Demas, J. N.; Flynn, C. M. *Anal. Chem.* **1976**, *48*, 353.

Table II. Spectral Data

complex	abs,^{a} $10^{-3}\nu_{max}$, cm^{-1} (ϵ_{max}, M^{-1} cm^{-1})					emission^b (77 K)		
						$10^{-3} \times$ ν_{max}, cm^{-1}	width at half-max, cm^{-1}	lifetime, μs
[Rh(2=phos)$_2$]ClO$_4$	20.7^c	24.7 (5580)	29.2 (5100)^d	31.8 (8400)		16.7	1970	30.4
[Rh(dpbe)$_2$]ClO$_4$	20.0^c	23.5 (5130)	30.7 (8260)^d	32.6 (11 380)		17.0	2320	21.5
[Rh(dpp)$_2$]PF$_6$		24.7 (2950)				13.4^e	2390^e	58.3^e
[Rh(dcpe)$_2$]PF$_6$	21.3^c	24.8 (5490)	29.5 (4300)^d	31.7 (5710)	35.2 (3680)	15.7	1910	50.1
[Rh(arphos)$_2$]PF$_6$	20.7^c	24.6 (4320)		31.2 (8470)		14.7	2180	49.1
[Rh(2=ars)$_2$]PF$_6$	20.7^c	24.9 (3530)	28.3 (5010)^d	30.6 (8600)		13.6	1950	75.8
[Rh(2=phos)(cod)]PF$_6$		22.4 (2590)		30.9 (6110)		14.2	2380	not found
[Ir(diphos)$_2$]ClO$_4$	19.0 (744)	22.6 (5250)		26.2 (5400)	31.5 (12 200)	17.0	1730	15
[Ir(2=phos)$_2$]ClO$_4$	19.0 (943)	22.6 (6450)		26.4 (6970)	31.4 (10 700), 31.9 (10 800)	18.3	500	10.7
[Ir(dpbe)$_2$]ClO$_4$	18.7 (526)	21.7 (4390)		25.5 (3390)	31.0 (7390)	17.9	450	6.3
[Ir(arphos)$_2$]PF$_6$	18.8 (284)	22.4 (1200)		25.6 (1330)	31.4 (4740)	16.2, 17.7^d	2710	15.4
[Ir(diphos)(cod)]PF$_6$	16.7 (465)	19.7 (2480)	20.4 (2010)^d	24.8 (3310)	31.8 (8500)	16.1^f	620	10.3
[Ir(2=phos)(cod)]PF$_6$	16.8 (505)	19.8 (2790)	20.4 (2340)^d	25.0 (3820)	31.8 (8900)	16.2^f	700	10.4
[Ir(dpbe)(cod)]PF$_6$	16.6 (498)	19.6 (2820)	20.2 (2510)^d	24.8 (3740)	31.5 (9170)	15.9^f	610	9.5

^{a} Room temperature in CH$_2$Cl$_2$ solution unless stated otherwise. ^{b} 16:4:1 ethanol-methanol-CH$_2$Cl$_2$ glass unless stated otherwise. ^{c} Obtained from excitation spectrum at 77 K in 16:4:1 ethanol-methanol-CH$_2$Cl$_2$ glass. ^{d} Shoulder. ^{e} Solid. ^{f} 650-cm^{-1} progression on band.
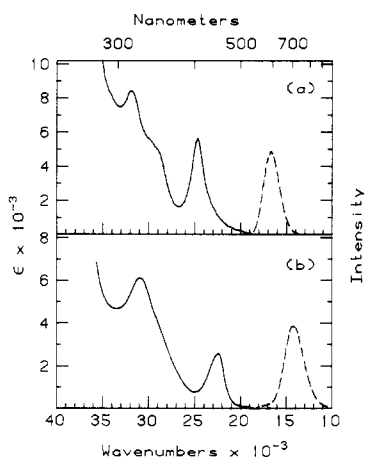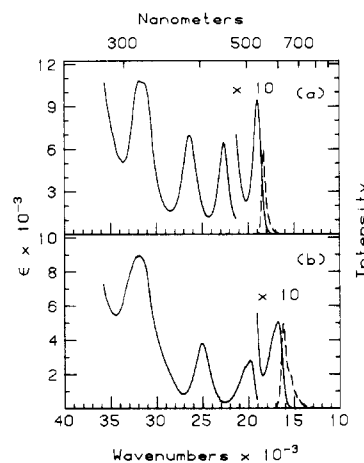

Figure 1. Room-temperature absorption spectra in dichloromethane (—) and 77 K emission spectra in 16:4:1 ethanol–methanol–dichloromethane (- - -) of (a) [Rh(2=phos)$_2$]ClO$_4$ and (b) [Rh(2=phos)(cod)]PF$_6$.

Figure 2. Room-temperature absorption spectra in dichloromethane (—) and 77 K emission spectra in 16:4:1 ethanol–methanol–dichloromethane (- - -) of (a) [Ir(2=phos)$_2$]ClO$_4$ and (b) [Ir(2=phos)(cod)]PF$_6$.

Figure 3. Emission excitation spectrum (—) and emission spectrum (- - -) of [Rh(2=phos)$_2$]ClO$_4$; emission excitation maxima (-·-→, ···>) and emission spectra (-·-, ···) of [Rh(arphos)$_2$]PF$_6$ and [Rh(2=ars)$_2$]PF$_6$, respectively. All spectra taken at 77 K in 16:4:1 ethanol–methanol–dichloromethane.

appeared homogeneous under microscopic inspection. Products from reactions using [RhCl(CO)$_2$]$_2$ as a starting material show no ν_{CO} IR stretching bands. The solids, with the exception of [Rh(2=ars)$_2$]PF$_6$ and particularly [Ir(arphos)$_2$]PF$_6$, appeared to be air stable. From the observation of exponential emission lifetimes and the coincidence of bands in the absorption and emission excitation spectra, we conclude that no trace impurities that contributed to the electronic spectroscopy were present in the samples. Thus, although we are unable to explain the poor analytical results, we believe that the samples were spectroscopically pure.

The ^{31}P NMR spectrum of [Rh(arphos)$_2$]PF$_6$ contained two doublets. The first doublet at 66.4 and 62.2 ppm (J_{Rh-P} = 151.4 Hz, relative to 85% H$_3$PO$_4$ and positive downfield) is assigned to the cis isomer (60%). The second doublet at 63.9 and 60.5 ppm (J_{Rh-P} = 124.5 Hz) is assigned to the trans isomer (40%).

Spectroscopy. The room-temperature absorption and 77 K emission data for the complexes are given in Table II. With the exception of the cod species, the absorption band maxima varied only slightly relative to the prototype [M(2=phos)$_2$]ClO$_4$ complexes shown in Figures 1a and 2a. The low-energy absorption band maxima of [M(2=phos)(cod)]PF$_6$ (Figures 1b and 2b) were red shifted ~2500 cm^{-1} relative to the bis-
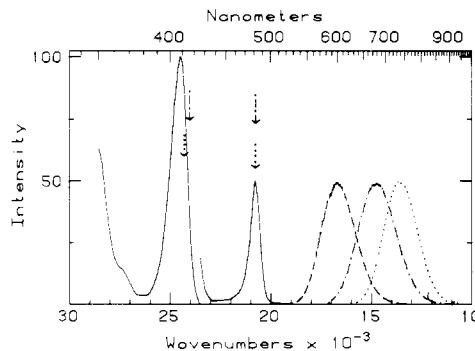
(2=phos) complexes as were the emission bands. In addition the extinction coefficients of the low-energy absorption bands of the cod complexes were significantly lower than the values for the analogous bis complexes. Another feature evident in Table II is the similarity of all the spectral data for the Ir(I)–cod complexes.
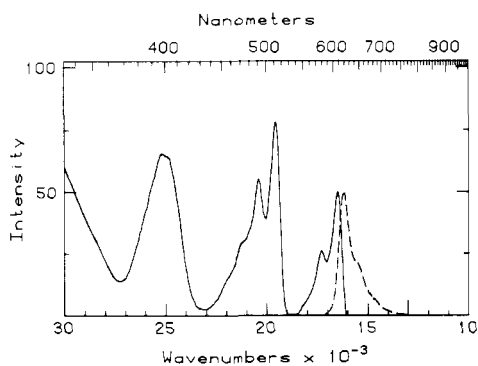
Figure 4. Emission excitation (—) and emission (- - -) spectra of [Ir(2=phos)(cod)]PF$_6$ at 77 K in 16:4:1 ethanol--methanol--dichloromethane.
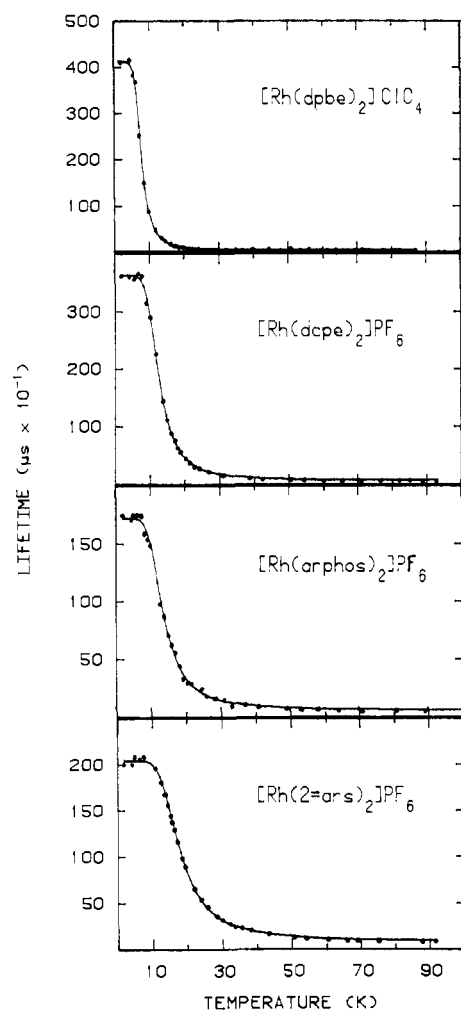

Figure 5. Temperature dependence of the lifetimes in 16:4:1 ethanol–methanol–dichloromethane and computer-generated fits for rhodium(I) complexes: ●, experimental values; —, "best-fit" computer-generated curves.
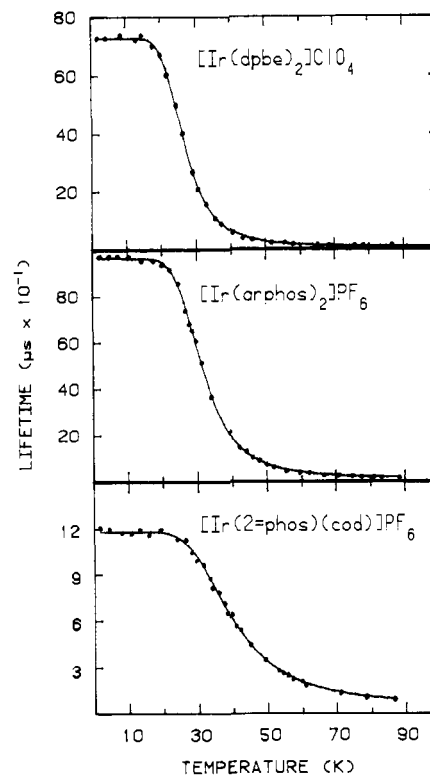

Figure 6. Temperature dependence of the lifetimes in 16:4:1 ethanol–methanol–dichloromethane and computer-generated fits for iridium(I) complexes: ●, experimental values; —, "best-fit" computer-generated curves.

Emissions from the Rh(I) complexes were broad and unstructured. As arsines were substituted for phosphines in the series [Rh(L–L)$_2$]$^+$ (L–L = 2=phos, arphos, 2=ars) the luminescence red shifted as shown in Figure 3. [Rh(dpp)$_2$]PF$_6$ displayed no emission in a glass but glowed intensely in the solid state. The low energy of the emission relative to the other complexes was probably not due to the change in medium since emissions recorded from glasses or the solid state generally differed in energy by 1000 cm^{-1} or less. The emission from [Rh(2=phos)(cod)]PF$_6$ was quite weak, prohibiting measurement of both the lifetime and the excitation spectrum.

Emission bands from the Ir(I) complexes were generally narrower than those from the Rh(I) complexes. For all the Ir(I)–cod systems, the luminescence band displayed a 650-cm^{-1} progression (Figure 2b). That from [Ir(arphos)$_2$]PF$_6$ displayed an anomalous shoulder on the high-energy side.

The low-energy band ($\sim$24000 cm^{-1}) in the absorption spectra of the Rh(I) complexes was considerably more narrow in the excitation spectra and a relatively weak band at low energy ($\sim$21000 cm^{-1}) was revealed (for example, see Figure 3). As in the case of the absorption bands this weak band was relatively insensitive to changes in the phosphine or arsine ligands; the corresponding excitation band maxima of [Rh(arphos)$_2$]PF$_6$ and [Rh(2=ars)$_2$]PF$_6$ differed from those of [Rh(2=phos)$_2$]ClO$_4$ by $\lesssim$300 cm^{-1} (Figure 3). No overlap occurred between this lowest energy excitation band and the emission band in any Rh(I) complex. The 77 K excitation spectra of solid samples obtained at high instrument sensitivity failed to reveal additional bands between those at $\sim$21000 cm^{-1} and the emission bands.

The excitation spectra of the Ir(I) complexes revealed no new bands not already seen in the absorption spectra. As shown in Figure 4, the 650-cm^{-1} progression observed in the emission bands of the Ir(I)–cod complexes was also observed in the two lowest energy excitation bands of these molecules. In contrast to the Rh(I) spectra, considerable overlap did exist between the lowest energy excitation band and the emission band for the Ir(I) complexes. The least overlap occurred for [Ir(diphos)$_2$]ClO$_4$ and [Ir(arphos)$_2$]PF$_6$.

Low-Temperature Lifetimes. The 77 K emission lifetimes are listed in Table I. As the temperature was lowered, the lifetimes increased dramatically as shown in Figures 5 and 6. Our method of analysis of the data, which has been developed previously,[18] assumes an emitting manifold of states. The physical assumptions are (a) each level in the emitting man-
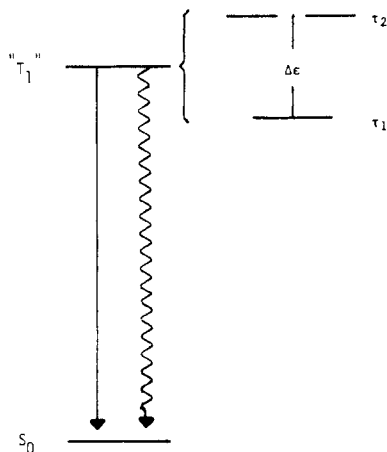
(18) Hager, G. D.; Crosby, G. A. *J. Am. Chem. Soc.* **1975**, *97*, 7031.

Figure 7. Diagram of the emission process and splitting of the triplet level.

Table III. Emitting Manifold Parameters for Complexes

complex	$\Delta\epsilon$, cm^{-1}	τ_1, μs	τ_2, μs
$[Rh(2{=}phos)_2]ClO_4{}^a$	37.8	5915	10.2
$[Rh(dpbe)_2]ClO_4$	33.0	4120	8.4
$[Rh(dcpe)_2]PF_6$	47.2	3630	16.3
$[Rh(arphos)_2]PF_6$	44.8	1719	15.0
$[Rh(2{=}ars)_2]PF_6$	57.6	2043	20.7
$[Ir(2{=}phos)_2]ClO_4{}^a$	143	999	0.77
$[Ir(dpbe)_2]ClO_4$	133	729	0.59
$[Ir(arphos)_2]PF_6$	151	966	1.00
$[Ir(2{=}phos)(cod)]PF_6$	140	118	0.79

^{a} τ_2 value listed represents decay time of entire degenerate level and is half that previously reported.[8]

ifold is coupled to the ground state by first-order processes with temperature-independent radiative and quenching rate constants and (b) Boltzmann equilibrium is established among the levels in times much shorter than the lifetime of the manifold.

A diagram of the emission process for the systems studied here is shown in Figure 7. The expression appropriate for describing the measured lifetime of these systems is given by

$$\tau(T) = [1 + 2\exp(-\Delta\epsilon/kT)]/[k_1 + 2k_2\exp(-\Delta\epsilon/kT)] \quad (1)$$

where $\tau(T)$ is the measured lifetime at temperature T, $\Delta\epsilon$ is the energy gap between the two levels in the emitting manifold, and k_1 and k_2 are the rate constants for depopulating the lower and higher levels, respectively, to the ground state. The temperature-dependent lifetime data were analyzed with a multiparameter least-squares curve-fitting computer program to find the three constants $\Delta\epsilon$, k_1, and k_2 contained in eq 1. The computer-generated fits are shown in Figures 5 and 6 and the results given in Table III. In eq 1 the second level in the emitting manifold has been assigned a degeneracy factor of 2. Although this degeneracy factor is not derivable from the experimental data, it is consistent with the proposed term assignments (vide infra). The inclusion of the degeneracy factor does not significantly affect the quality of the computer fit or the derived values of the parameters. It should be noted that the τ_2 values in Table III represent the lifetime of the entire level.

Low-Temperature Emissions. The emission spectra of the Rh(I) complexes did not change significantly over the temperature region studied (1.8–90 K). In contrast, the spectra of $[Ir(2{=}phos)_2]ClO_4$,[8] $[Ir(dpbe)_2]ClO_4$, and $[Ir(2{=}phos)(cod)]PF_6$ varied markedly with temperature. The high-temperature spectrum (>30 K) of $[Ir(2{=}phos)_2]ClO_4$ displayed a maximum at 18 360 cm^{-1}, whereas the low-temperature spectrum (<20 K) maximized at 17 860 cm^{-1}. At temperatures
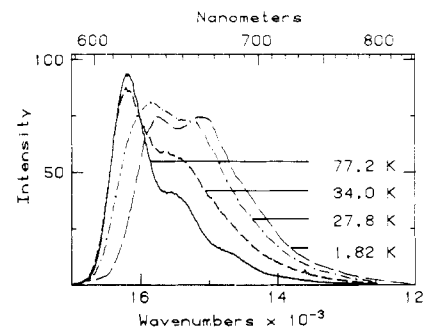

Figure 8. Emission spectra of $[Ir(2{=}phos)(cod)]PF_6$ in 16:4:1 ethanol–methanol–dichloromethane at the indicated temperatures. Relative intensities between spectra are arbitrary.
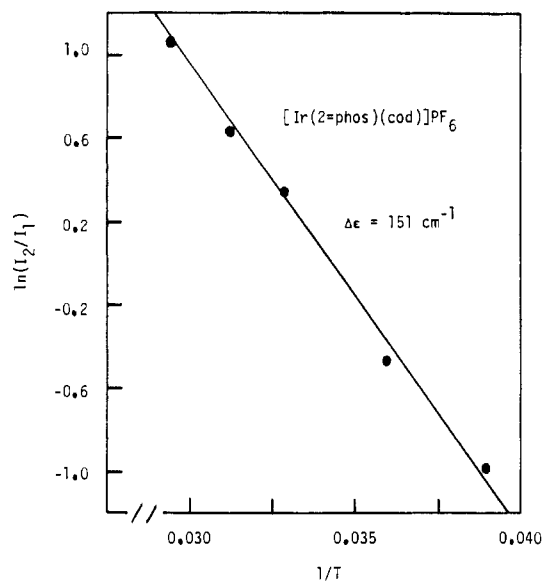

Figure 9. Temperature dependence of the logarithm of the ratio of the intensity of the high-temperature emission spectrum to the low-temperature emission spectrum of $[Ir(2{=}phos)(cod)]PF_6$.

between 20 and 30 K, the spectra were weighted superpositions of the two extremes.

This spectral change, analyzed previously,[8] was described by

$$\ln (I_2/I_1) = -\Delta\epsilon/kT + \ln (2k_{2r}/k_{1r}) \quad (2)$$

where I_1 and I_2 are the integrated emission intensities from levels 1 and 2, respectively, $\Delta\epsilon$ is the energy gap between the levels, and k_{1r} and $2k_{2r}$ are the radiative rate constants for depopulating levels 1 and 2, respectively. If k_{1r} and k_{2r} are temperature independent, eq 2 predicts a linear relationship between $\ln (I_2/I_1)$ and $1/T$, with a slope equal to $\Delta\epsilon$. To employ eq 2 it is necessary to correct the intensity data for the overlap of spectra from the high- and low-temperature extremes. We also assumed that the integrated emission intensity was proportional to the intensity at any chosen wavelength. The plot of $\ln (I_2/I_1)$ vs. $1/T$ yielded a linear least-squares value for $\Delta\epsilon$ of 141 cm^{-1} [8] in excellent agreement with the value of 143 cm^{-1} obtained from the temperature vs. lifetime data (Table III).

The change in the emission spectrum of $[Ir(dpbe)_2]ClO_4$ with temperature was similar to that previously reported for $[Ir(2{=}phos)_2]ClO_4$,[8] and we conclude that the two-level scheme is also analogous. The effect of temperature upon the emission spectrum of $[Ir(2{=}phos)(cod)]PF_6$ is shown in Figure 8. Analysis of the data produced the $\ln (I_2/I_1)$ vs. $1/T$ plot shown in Figure 9 and a $\Delta\epsilon$ value of 151 cm^{-1}, in good agreement with the value of 140 cm^{-1} obtained from the lifetime analysis (Table III).

Discussion

Geoffroy et al.[2] have given a simplified molecular orbital scheme for the complexes with D_{4h} microsymmetry. The orbitals pertinent to the discussion here are the highest occupied orbital, nd_{z^2} (a_{1g}), and the lowest unoccupied orbital, which they indicate to be an admixture of π_L (a_{2u}), composed of p_z orbitals on the P or As atoms and a metal $(n + 1)p_z$ orbital. We adopt the same scheme here but prefer to view the π_L (a_{2u}) orbital as a linear sum of P(As) d orbitals oriented in vertical planes containing the z axis and diagonals of the square. In this picture the P(As) atoms are pseudotetrahedral as demanded by the crystal structure data,[19] and the p_z orbitals are unavailable for generating a π_L (a_{2u}) orbital. Irrespective of the choice of basis set the symmetry conditions are the same, however. Previously,[2-5] the lowest energy transitions were assigned to metal-to-ligand charge transfer, $nd_{z^2} \rightarrow \pi_L$, with the $(n + 1)p_z$ orbital playing an undetermined role in the excited states. In consonance with earlier studies,[2-6] we assign the weak lowest energy absorption band observed in the excitation spectra of the Rh(I) complexes and in both the absorption and excitation spectra of the Ir(I) complexes to the $^1A_{1g} \rightarrow {^3A_{2u}}$ ($a_{1g} \rightarrow a_{2u}$) transition. The emission band is assigned to the corresponding phosphorescence. Also in agreement with others, we assign the next higher energy band observed in the absorption and excitation spectra of all the complexes to the $^1A_{1g} \rightarrow {^1A_{2u}}$ ($a_{1g} \rightarrow a_{2u}$) transition.

The relative insensitivity of the energy of the absorption bands to changes in the diphosphine ligand indicates that the lowest unoccupied molecular orbital is not significantly delocalized onto the rings bound to the phosphorous atoms or onto the linkage between the phosphorous atoms but is restricted to the phosphorous atoms and/or the metal center. More striking is the insensitivity to replacement of phosphorus with arsenic. For the bis(arphos) complexes the symmetry is reduced and a mixture of cis and trans isomers exists; yet no significant shifts in energy or splitting of absorption bands is observed. These results argue strongly in favor of significant $(n + 1)p_z$ character in the lowest unoccupied orbital since a metal localized state would be expected to be less sensitive to variations in the ligands than a charge-transfer state.

The only ligand change that does produce substantial shifts in the energies of the absorption bands is replacement of a diphosphine with cod. The consequent red shift of all the lower energy spectral features indicates either a destabilization of all the d orbitals relative to the lowest unoccupied orbital π_L:($n + 1$)p_z or stabilization of the π_L:($n + 1$)p_z orbital relative to the d orbitals. We opt for the former case. Although crystal structure data are not available for the complexes studied here, data for the related complexes [Rh(diphos)$_2$]ClO$_4$[19] and [Rh(Ph$_2$PCH(CH$_3$)CH(CH$_3$)PPh$_2$)(cod)]ClO$_4$[20] reveal average Rh–P distances of 2.306 and 2.271 Å, respectively. The reduced distance in the cod complex may be due to relief of steric interactions between the phenyl rings on opposing diphosphines. By crystal field arguments, the closer approach of the diphosphine ligand to the metal center would be expected to destabilize the d orbitals.

The 650-cm^{-1} progression observed on the $^1A_{1g} \rightarrow {^{1,3}A_{2u}}$ absorptions and corresponding phosphorescences of the Ir(I)–cod complexes is probably vibrational in nature although we are unable to assign it. As in the case of the bis(arphos) complexes, no effects are observed in the spectra that can be attributed to the reduction of symmetry from D_{4h} to C_{2v}. The reduction in ϵ values, in most cases $\sim 50\%$, upon replacement of a diphosphine with cod, supports the charge-transfer nature of these transitions. The similarity of all the spectral features

of the Ir(I)–cod complexes suggests that none of the charge density in the excited state is localized on the linkage between the phosphorous atoms. The small Stokes shifts indicate that the ground- and excited-state geometries are very similar.

The large Stokes shifts observed in the emission spectra of the Rh(I) complexes imply a substantial distortion of the systems in the excited state. Geoffroy et al.[2] suggested that the excited state contained a small admixture of one or more d–d states leading to a tetrahedral distortion. If this were the case, the destabilization of the d orbitals in [Rh(2=phos)(cod)]PF$_6$ (vide supra) should reduce the d–d mixing in the lowest excited states relative to the bis complexes and result in a reduced Stokes shift, contrary to our results. In addition, the excitation polarization ratio study by Andrews[6] indicated that no symmetry reducing distortions occurred in the low-energy excited states of the [M(L–L)$_2$]$^+$ [M = Rh(I), Ir(I); L–L = diphos, 2=phos] complexes. Consequently the distortion must involve a symmetric expansion or contraction of the metal–ligand core. The increase in the Stokes shift as the larger arsenic is substituted for phosphorus and the increase upon adding a carbon to the chain bridging the phosphorus atoms (substituting dpp for 2=phos) suggest that the distortion may be linked to steric rather than electronic factors.

The exceptionally small Stokes shifts observed for most of the Ir(I) complexes (~ 300 cm^{-1}, absorption maxima taken from 77 K excitation spectra) and mirror-image relationship between excitation and emission bands indicate a virtually undistorted excited state. We are unable to explain the exceptions, [Ir(diphos)$_2$]ClO$_4$ and [Ir(arphos)$_2$]PF$_6$, or the dramatic difference in Stokes shifts between the Rh(I) and Ir(I) complexes.

Low-Temperature Studies. The satisfactory fits of the lifetime vs. temperature data support the physical assumptions used in our analysis. In addition the observation of distinct high- and low-temperature spectra for some of the Ir(I) complexes and the good fit of the data clearly indicate the presence of two levels. We therefore opt for a model in which the change in lifetime with temperature is caused by a change in the relative population of the two levels as opposed to a model in which the change in lifetime is caused by a change with temperature in one or both the radiative and quenching rate constants of a single level.

Analysis of the lifetime vs. temperature data in all cases yields a higher level with a lifetime much shorter than that of the lower level, indicating that emission from the higher level is a partially allowed transition, whereas emission from the lower level is forbidden.[21] The free-ion spin–orbit coupling constant for Rh(I), ζ_{4d}, is 1200 cm^{-1}, whereas for Ir(I) ζ_{5d} is ~ 4000 cm^{-1}.[22] These values fall into approximately the same ratio as $\Delta\epsilon$ of analogous Rh(I) and Ir(I) complexes studied here. We infer that the splitting mechanism is spin–orbit coupling. In view of the large free ion spin–orbit coupling values for Rh(I) and Ir(I), this splitting of the lowest triplet appears to be unusually small. For a $^3A_{2u}$ term, however, the splitting should vanish in first order because of the nondegenerate nature of the A_{2u} orbital. With our assignment one must invoke higher order interactions to account for the observed energy gaps.

Because of the obvious similarity of the lifetimes of the Rh(I) and Ir(I) decay curves with temperature, we also infer that there is negligible d–d character in the Rh(I) excited configuration. Geoffroy et al.[2] assigned the emission from [M(L–L)$_2$]$^+$ [M = Rh(I), Ir(I); L–L = diphos, 2=phos] at

(19) Hall, M. C.; Kilbourn, B. T.; Taylor, K. A. *J. Chem. Soc. A* **1970**, 2539.
(20) Ball, R. G.; Payne, N. C. *Inorg. Chem.* **1977**, *16*, 1187.
(21) The total emission intensity remained the same or decreased as the temperature was lowered. We infer that the quantum yield of the lower level was equal to or less than, respectively, that of the higher level.
(22) Griffith, J. S. "The Theory of Transition Metal Ions"; Cambridge University Press: London, 1964; p 113.

77 K as arising from the dipole allowed E_u spin–orbit component of the $^3A_{2u}$ term (D_{4h} symmetry). This leads us to assign the shorter lived higher energy emitting level as an E_u state (thus doubly degenerate) and the lower energy emitting level as the forbidden A_{1u} spin–orbit component derived from the $^3A_{2u}$ term. In the case of the bis(arphos) complexes (cis isomer, C_{2v}; trans isomer, D_{2h}) and cod complexes (C_{2v}), the lowering of symmetry splits the degenerate E_u level into two dipole-allowed components in the lower symmetry groups. In the temperature vs. lifetime data and also the spectral data, we see no evidence for the splitting of the E_u level in these complexes. Apparently the levels are accidentally degenerate or separated by only a few wavenumbers.

Trends in the data presented in Table III allow us to draw a number of conclusions concerning the nature of the lowest emitting term of these complexes. Most apparent is the larger $\Delta\epsilon$ values and lesser τ values of the Ir(I) species compared to those of Rh(I). These values reflect the greater spin–orbit coupling constant of Ir(I); this is also manifested in the larger extinction coefficients of the triplet absorption bands of all the Ir(I) complexes. We also ascribe the increase in $\Delta\epsilon$ as arsenic is substituted for phosphorus to the larger spin–orbit coupling constant of the former atom. This dependence of $\Delta\epsilon$ on the nature of the chelated atom clearly demonstrates the involvement of these atoms in the excited triplet. One expects the aromatic linkage between phosphorous atoms in the dpbe ligand to delocalize some of the charge density off the phosphorus atoms; a correspondingly slightly reduced $\Delta\epsilon$ value [ζ(phosphorus) $\gg$ ζ(carbon)] is found. Conversely, the replacement of the phenyl rings in diphos with cyclohexyl groups in the dcpe ligand should keep the charge density on the phosphorus atoms; $\Delta\epsilon$ also increases. Conclusions drawn from trends in the τ values are risky since these parameters are

related to the radiative lifetimes by the quantum yields, which we do not know. The only τ value that stands out is the relatively short τ_1 value for [Ir(2=phos)(cod)]PF$_6$. Perhaps the replacement of a phosphine with cod facilitates geometrical distortions that reduce the forbiddenness of the lower level.

We have established the existence of a two-level emitting manifold in these complexes from analysis of the lifetimes vs. temperature and from spectral band-shape data. The substantial reduction of the molar extinction coefficients upon replacement of a diphosphine with cod and the effect on $\Delta\epsilon$ upon replacing P with As in the ligands demonstrate a charge-transfer component in the low-energy states. This component appears to be predominantly localized on the P or As atom. Although not yet quantified, the metal-localized component of the low-energy excited states is demonstrated by the relative insensitivity of the spectral features to changes in ligands, particularly replacement of phosphorus with arsenic, and the absence of measurable splitting of degenerate levels upon reducing the core symmetry. The 2500-cm^{-1} red shift of all the spectral features upon replacement of a diphosphine with cod is attributed to destabilization of the d orbitals due to closer approach of the diphosphine to the metal center.

Registry No. [Rh(2=phos)$_2$]ClO$_4$, 57749-19-6; [Rh(dpbe)$_2$]ClO$_4$, 80340-14-3; [Rh(dpp)$_2$]PF$_6$, 80340-15-4; [Rh(dcpe)$_2$]PF$_6$, 80340-17-6; [Rh(arphos)$_2$]PF$_6$, 80340-18-7; [Rh(2=ars)$_2$]PF$_6$, 60646-26-6; [Rh(2=phos)(cod)]PF$_6$, 80340-19-8; [Ir(diphos)$_2$]ClO$_4$, 15685-14-0; [Ir(2=phos)$_2$]ClO$_4$, 36390-40-6; [Ir(dpbe)$_2$]ClO$_4$, 80340-21-2; [Ir(arphos)$_2$]PF$_6$, 80375-21-9; [Ir(diphos)(cod)]PF$_6$, 61817-48-9; [Ir(2=phos)(cod)]PF$_6$, 80340-22-3; [Ir(dpbe)(cod)]PF$_6$, 80340-24-5.

Contribution from the Istituto di Teoria e Struttura Elettronica e Comportamento Spettrochimico dei Composti di Coordinazione del CNR, Area della Ricerca di Roma, Monterotondo Stazione, Roma, Italy

EPR Spectra of Eight-Coordinated Complexes of the Early Transition Metals with Sulfur and Selenium Donor Ligands. 3.[1,2] Vanadium(IV) and Niobium(IV) Dithio- and Diselenocarbamates

D. ATTANASIO,* C. BELLITTO,* A. FLAMINI,* and G. PENNESI

Single-crystal and powder EPR studies of the eight-coordinated complexes tetrakis(N,N-diethyldithiocarbamato)vanadium(IV), tetrakis(N,N-diethyldithiocarbamato)niobium(IV), and tetrakis(N,N-diethyldiselenocarbamato)vanadium(IV), diluted in the diamagnetic Ti(IV) analogues, are reported. Two, chemically inequivalent, crystallographic sites are present in the unit cell of the two isomorphous host compounds. They are differently populated by the paramagnetic ions, the most asymmetric site accounting for about 75% of the total V(IV) or Nb(IV) concentration. All the different EPR signals arise from discrete eight-coordinated species, with a molecular geometry close to the ideal triangular dodecahedron (D_{2d}). The mixing coefficients in a ground-state orbital of the type $a|x^2 - y^2\rangle - b|z^2\rangle$ have been obtained from the experimental results and related to the deviation from pure D_{2d} symmetry. However, no simple relationship could be found between this distortion and the type of ligands or metal ion involved. Low-intensity satellite lines have been observed in the spectrum of V/Ti(Et$_2$dsec)$_4$ and attributed to the hyperfine coupling of the unpaired electron with four different selenium nuclei. No splitting from the other four selenium ligands could be observed. This result has been related to the inequivalence of the A and B ligand sites of the dodecahedron and, specifically, to the different overlap between the metal ion ground-state orbital and the ligand $\pi_\perp$ orbitals.

Introduction

As a continuation of our interest in eight-coordinated complexes of sulfur and selenium donor ligands, we report here a single-crystal and powder EPR study of tetrakis(N,N-di-

ethyldithiocarbamato)vanadium(IV), V(Et$_2$dtc)$_4$, tetrakis-(N,N-diethyldithiocarbamato)niobium(IV), Nb(Et$_2$dtc)$_4$, and tetrakis(N,N-diethyldiselenocarbamato)vanadium(IV), V-(Et$_2$dsec)$_4$, substitutionally diluted in the diamagnetic Ti(IV) analogues.

In a previous EPR work on eight-coordinated dithiocarboxylato complexes,[1,2] with the same metal ions, we have shown that these compounds have an essentially $|x^2 - y^2\rangle$

(1) Attanasio, D.; Bellitto, C.; Flamini, A. *Inorg. Chem.* **1980**, *19*, 3419.
(2) Attanasio, D.; Bellitto, C.; Flamini, A.; Pennesi, G. *Chem. Phys. Lett.* **1980**, *72*, 307.